

# Ionic liquids and cyclodextrin inclusion complexes: limitation of the affinity capillary electrophoresis technique

Nadine Mofaddel<sup>1</sup> · Sophie Fourmentin<sup>2</sup> · Frédéric Guillen<sup>1,3</sup> · David Landy<sup>2</sup> · Géraldine Gouhier<sup>1</sup>

Received: 7 July 2016 / Revised: 22 August 2016 / Accepted: 7 September 2016 / Published online: 5 October 2016  
© Springer-Verlag Berlin Heidelberg 2016

**Abstract** The state of the art of inclusion complex formation between cyclodextrins and ionic liquids is reported. Mechanisms, stoichiometries, and binding constants are summarized and classified by anion. We investigated the supra-molecular interactions between the  $\beta$ -cyclodextrin cavity and six ionic liquids based on 1-dodecyl-3-methylimidazolium by affinity capillary electrophoresis and compared the results with those obtained by isothermal titration calorimetry. We show that the presence of basic or acidic buffers leads to a metathesis reaction, underlining the limitation of the affinity capillary electrophoresis technique.

**Keywords** Affinity capillary electrophoresis · Binding constants · Cyclodextrin · Ionic liquid · Isothermal titration calorimetry

## Introduction

Cyclodextrins are macrocyclic molecules called  $\alpha$ -CD,  $\beta$ -CD, or  $\gamma$ -CD when they are composed of six, seven, or eight

**Electronic supplementary material** The online version of this article (doi:10.1007/s00216-016-9931-z) contains supplementary material, which is available to authorized users.

✉ Géraldine Gouhier  
geraldine.gouhier@univ-rouen.fr

<sup>1</sup> UNIROUEN, INSA Rouen, CNRS, COBRA (UMR 6014), Normandie Université, 1 rue Tesnière, 76000 Rouen, France

<sup>2</sup> Unité de Chimie Environnementale et Interactions sur le Vivant (UCEIV, EA 4492), SFR Condorcet FR CNRS 3417, ULCO, 59140 Dunkerque, France

<sup>3</sup> SPCMIB, CNRS-UMR 5068, Université Toulouse III - Paul Sabatier, 118 route de Narbonne, 31062 Toulouse Cedex 9, France

$\alpha$ -(1 $\rightarrow$ 4) glucopyranose units respectively [1]. In an aqueous medium CDs adopt a truncated cone shape that constitutes a large and well-defined cavity (host) that can welcome an organic molecule (guest). Such host–guest inclusion complexes improve the weak solubility and bioavailability of the guest in the medium and find applications in vectorization of drugs, for example. The primary and secondary hydroxyl groups form two crowns with hydrophilic character, whereas the internal cavity constituted of hydrogen atoms (H-3, H-5, H-6) and interglycosidic oxygen (O-4) is hydrophobic. CDs are soluble in water because of the presence of free and labile water molecules forming a hydration sphere. Even after dehydration, water molecules stay inside the cavity. In an aqueous medium, the substitution of a lipophilic guest for the inner water molecules to form an inclusion complex needs energy and repulsive and attractive interactions (polar–apolar) inside the cavity. Hydrophobic interaction is the main driving force for the formation of the complex, but the size matching between the host and the guest is also an important parameter. Weak interactions such as hydrogen and van der Waals bonding allow a thermodynamic equilibrium between associated and dissociated forms that can be characterized by an association constant  $K$ . Many methods have been used to determine this value and the stoichiometry of the complex, such as conductimetry, competitive fluorescence, affinity capillary electrophoresis (ACE), UV–visible spectroscopy, IR spectroscopy, isothermal titration calorimetry (ITC), nuclear magnetic resonance (NMR) spectroscopy, high-resolution mass spectrometry (HRMS), and X-ray diffraction [2].

Ionic liquids (ILs) are polar liquid salts with exceptionally low melting points (by convention below 100 °C, but frequently below room temperature) [3, 4]. Most of them have high thermal and chemical stability, and their low vapor pressure reduces drastically their toxicity risk from inhalation and prevents inflammation. In addition, they display interesting

solvating properties that depend on the nature of the cation and anion, enabling them to dissolve a large number of organic or inorganic compounds. They are therefore considered as a promising alternative to volatile organic solvents. Some ILs are especially good solvents for glucose and cellulose and improve the dissolution of CDs. These original properties also lead to supramolecular interactions with all other external dissolved molecules.

The CD–IL combination is an interesting couple with a wide range of applications in supramolecular chemistry thanks to no covalent interaction with other molecules in contact. In addition to the enhancement of stabilization and solubilization properties [5, 6], the CD–IL association has recently been applied in polymer chemistry, molecular devices, and nanoscience. CD–IL polymeric complexes appear useful to remove organic and inorganic contaminants from water [7–9]. The inclusion of the anions of ILs in  $\beta$ -CD water-insoluble copolymers results in a significant change in the thermal and solution properties by causing a switch from water insolubility to water solubility [10]. Synergistic participation of inclusion complexes with use of imidazolium surfactants can provide a new micellar catalysis environment [11]; alternatively, these inclusion complexes can also aggregate into vesicles, forming temperature-induced reversible-transition sheet-like hydrogel [12, 13]. A robust and flexible Velcro-type polymer was recently synthesized via surface modification of polyIL (PIL) membranes with ferrocene and  $\beta$ -CD moieties, which act as the hooks and loops by host–guest recognition between PIL– $\beta$ -CD and PIL–ferrocene membranes [14]. All these new supramolecular properties should find applications in biochemistry and in the design of smart materials.

The interactions between IL and CD are also important in analytical chemistry to improve the separation as stationary or mobile phases for high-pressure liquid chromatography [15], gas chromatography [16], and ACE [17].

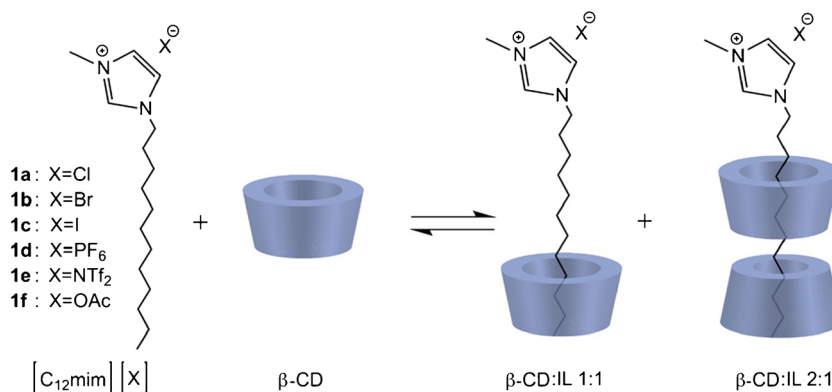
We have studied six ILs obtained by the association of the 1-dodecyl-3-methylimidazolium cation ( $C_{12}mim^+$ ) with six anions—chloride ( $Cl^-$ ), bromide ( $Br^-$ ), iodide ( $I^-$ ), triflimide ( $NTf_2^-$ ), hexafluorophosphate ( $PF_6^-$ ), and acetate ( $AcO^-$ )—by ACE and ITC experiments (Fig. 1). No data have been reported in the literature for these ILs. Indeed, only one systematic ACE study on chiral separation properties of other cations, such as phosphonium, sulfonium, cystinium, ammonium, and guanidinium salts, has been reported [18]. Electrostatic repulsion of the imidazolium ring charge will favor the interaction with the long tail of the ILs, and the effect of the anion will be then underlined.  $\beta$ -CD was selected because of its better inclusion property and its greater use as a host in the research and industry domains. No systematic investigation using the same cation and various anions has been reported. This study aimed to quantify their influence on the stability of the inclusion complexes. We compare the results

obtained by ACE and ITC, draw conclusions on the limitations of the techniques, and suggest experimental adjustments.

### Cyclodextrin–ionic liquid inclusion complexes: mini review

Understanding the interactions between these two partners is fundamental to design the best combination to develop new applications. Several studies have been dedicated to the effects on macromolecular properties of the association of ILs (especially containing an imidazolium cation) and CDs. The interaction between IL and CD was suspected in 2002 by Tran and De Paoli Lacerda [19], who observed by near-IR spectroscopy a decrease of the association constant for phenol and  $\alpha$ -CD,  $\beta$ -CD, and  $\gamma$ -CD in the presence of 1-butyl-3-methylimidazolium chloride,  $[C_4mim][Cl]$ . It was concluded that such behavior has to be taken into account before ILs are used as an analyte. In 2005 Gao et al. [20] observed in the  $^1H$  NMR spectrum shifts of the protons of the internal  $\beta$ -CD cavity in the presence of 1-butyl-3-methylimidazolium hexafluorophosphate,  $[C_4mim][PF_6]$ . From these preliminary results, they suggested an inclusion of imidazolium cation located in the narrower part of the CD cone with a 1:1 stoichiometry. The first association constants of the inclusion complexes of  $\beta$ -CD– $[C_4mim][X]$  (X is Cl,  $BF_4^-$ , or  $PF_6^-$ ) were calculated from conductivity measurements, NMR analysis, or fluorescence measurements by competition with an indole structure (Table 1, entries 4, 8, and 12 respectively) [21]. He and Shen [21] classified the strength of the interaction between the anions and  $\beta$ -CD in the following order:  $PF_6^- \gg BF_4^- > Cl^-$ . In 2010 Rak et al. [22] definitively closed the discussion about the location of the anion in  $[C_4mim][PF_6]$  by means of a nuclear Overhauser enhancement spectroscopy experiment by concluding that a 1:1 CD–anion complex was formed. The study was extended with various carbon tails with from eight carbon atoms ( $C_8$ ) to two carbon atoms ( $C_2$ ), and the following competition order was suggested:  $C_8 > C_6 > PF_6^- > C_4 > C_2$ . One year later the study was extended to  $[C_nmim][PF_6]$  ILs with  $n = 2–8$ , and two equilibrium states were proposed to explain the formation of 1:1 and 2:1 CD–IL complexes thanks to the formation of separated ion pairs [23]. Weak interactions between  $[C_4mim][BF_4^-]$  and  $[C_8mim][BF_4^-]$  and  $\alpha$ -CD,  $\beta$ -CD, and  $\gamma$ -CD were described by means of ITC, UV spectroscopy, NMR spectroscopy, and conductivity measurements [24, 25]. The presence of 1:1 and 1:2 CD–IL stoichiometries (except with  $\alpha$ -CD) was determined by inclusion of one or two alkyl chains inside the cavity. The formation of an inclusion complex of triflimide anion was established with the 1:1  $\beta$ -CD–vinylimidazolium triflimide complex during a polymerization reaction study [26].  $^{19}F$  NMR analysis proved the total implication of the counterion  $NTf_2^-$ , leading to a naked cationic monomer ready for use.

**Fig. 1** Equilibrium pattern and possible structures of inclusion complexes in the  $\beta$ -cyclodextrin ( $\beta$ -CD)–ionic liquid (IL) system.  $Ntf_2$  triflimide



When the chain linked to the imidazolium cation has more than ten carbon atoms, the complexation mechanism changes. In this case the lipophilicity of the tail becomes stronger than the inclusion power of the organic anion, leading to a new equilibrium pattern. A 1:1  $\beta$ -CD- $[C_{12}mim][BF_4]$  inclusion complex was recently identified by <sup>1</sup>H NMR analysis and confirmed by Fourier transform IR spectroscopy and differential scanning calorimetry [27]. The antimicrobial activity of this IL is preserved after complexation, and the gradual delivery of the antimicrobial agent resulted in a threefold reduction of the acute toxicity in comparison with the neat compound. Gao et al. [28, 29] reported two-dimensional NMR studies of the formation of the  $\beta$ -CD- $[C_{12}mim][PF_6]$  inclusion complex. They suggested two stoichiometries: 1:1 with the imidazolium cycle above the larger rim of the  $\beta$ -CD and a head–tail 1:2  $\beta$ -CD–IL complex with two carbon chain going across the cavity in the reverse position (Fig. 1). No association constant was reported. He et al. [30] confirmed the inclusion of the NTf<sub>2</sub><sup>-</sup> counterion of  $[C_{12}mim][NTf_2]$  inside the cavity of the macrocycle. According to He et al., the association strength between CD and various anions and cations follows the order  $NfO^- > C_{12}mim^+ > NTf_2^- \sim AdCO_2^- \sim C_{10}mim^+ > C_8mim^+ > C_6mim^+ \sim PF_6^- > BF_4^- > C_4mim^+ > Cl^-$ . This investigation was extended with chain lengths ranging from 2 to 12 carbon atoms by fluorescence measurements, ITC, IR spectroscopy, and HRMS (Table 1, entries 15–18) [31]. All the results showed a stoichiometry of 1:1 CD–IL for  $[C_2mim][NTf_2]$  to  $[C_6mim][NTf_2]$  and 2:1 CD–IL for  $[C_8mim][NTf_2]$  to  $[C_{12}mim][NTf_2]$ . A multiple equilibria interaction pattern illustrated by two paths of complexation was then reported to explain the various inclusion possibilities. Two-dimensional NMR nuclear Overhauser enhancement spectroscopy of the 1:1  $\beta$ -CD- $[C_{12}mim][NTf_2]$  complex proved that the methylene group of the C<sub>12</sub> chain close to the imidazolium cycle did not interact with the CD rim and was positioned far away from the cavity [31]. Recently a molecular dynamics study confirmed the preferential stabilization with this hydrophobic tail embedded within the  $\beta$ -CD and localized the head group at approximately 11 Å from the primary rim, mainly driven by hydrophobic interactions [32].

Funasaki et al. [33] suggested a head-to-head orientation with an  $\alpha$ -CD dimer from analysis of rotating frame Overhauser enhancement spectroscopy spectra.

In the case of the inclusion of the fluorinated anion, the negative charge of the fluoride is transferred out of the cavity. Thus the complexation between IL and CD is a function of the hydrophobicity and the size matching of the cation and the anion as exemplified by ITC studies and molecular modeling with fluorinated chains [34].

The formation of the inclusion complex between IL and CD needs favorable conditions and a few steps. When contacted, the initial highly ordered and solvated states (guest and host separated) undergo (1) perturbation resulting in the loss of the inner water molecules present inside the cavity of the CD, (2) inclusion of the lipophilic guest by a hydrophobic effect, and finally (3) formation of hydrogen and van der Waals bonds. The global order of the system is then improved because of the final restricted conformational freedom. These cumulative modifications generate global variation of enthalpy and entropy. A disorder process leads to a favorable entropic gain and positive  $\Delta S$ . The desolvation step occurring in the course of the binding is slightly endothermic and increases the entropy. Van der Waals guest–host interactions are characterized by negative enthalpy.

Neat ILs have a nanostructured supramolecular network with a polar region and a nonpolar region [35]. In an aqueous medium, associated ion pairs appear, and at high dilution ion pairs mainly dissociate into separated cation and anion.

The passage between these different states also needs energy and modifies the interactions with water molecules and so the solubility of the mixture. For halide anions the water molecules are more coordinated, producing a stronger ion pair and forcing them to stay close to the imidazolium cation as a contact ion pair and far away from the CD cavity; more energy is necessary to break this ionic interaction [36]. Halide counterions have a smaller volume (24 Å<sup>3</sup>, 31 Å<sup>3</sup>, and 42 Å<sup>3</sup> for Cl<sup>-</sup>, Br<sup>-</sup>, and I<sup>-</sup> respectively) and no variation of the constant or thermodynamic data was observed, proving similar repulsion of these anions from the cavity (Table 1, entries 6 and 7). The hydrophilicity of these counteranions stabilizes the shell of the

**Table 1** Association constants reported in the literature for the formation of inclusion complexes between  $\beta$ -cyclodextrin and various ionic liquids classified by counteranion

Entry	Species	$K$ ( $M^{-1}$ )	Method
1	NaBF <sub>4</sub>	10 ± 2	Fluo [34]
2	KPF <sub>6</sub>	100 ± 1	Fluo [23]
		163 ± 2	Fluo [23]
		120 ± 1	ITC [22]
		85 ± 5	ITC [34]
		2490 ± 42	Fluo [31]
3	LiNTf <sub>2</sub>	2836 ± 116	ITC [31]
		0	ITC [22]
4	[C <sub>4</sub> mim][Cl]	8 ± 0.1	Fluo [21]
		0	ITC [22]
5	[C <sub>6</sub> mim][Cl]	90 ± 12	ITC [34]
6	[C <sub>8</sub> mim][Cl]	624 ± 43	ITC [34]
7	[C <sub>8</sub> mim][Br]	672 ± 50	ACE [37]
8	[C <sub>4</sub> mim][BF <sub>4</sub> ]	31 ± 1	Fluo [21]
		0	ACE [39]
9	[C <sub>10</sub> mim][BF <sub>4</sub> ]	3038 ± 290	ACE [39]
10	[C <sub>12</sub> mim][BF <sub>4</sub> ]	10,994 ± 600	ACE [37]
11	[C <sub>2</sub> mim][PF <sub>6</sub> ]	121 ± 2	Fluo [23]
		170 ± 5	ITC [23]
12	[C <sub>4</sub> mim][PF <sub>6</sub> ]	140 ± 3	Fluo [21, 23]
		159 ± 3	Fluo [21, 23]
		110 ± 10	Conductimetry [21]
		99 ± 6	<sup>19</sup> F NMR [21]
		84 ± 1	ITC [22]
13	[C <sub>6</sub> mim][PF <sub>6</sub> ]	189 ± 5	ITC [23]
		371 ± 15	Fluo [23]
14	[C <sub>8</sub> mim][PF <sub>6</sub> ]	401 ± 3	ITC [23]
		1177 ± 95	Fluo [23]
15	[C <sub>2</sub> mim][NTf <sub>2</sub> ]	119,936 ± 7340	ITC [23]
		3255 ± 172	Fluo [31]
16	[C <sub>4</sub> mim][NTf <sub>2</sub> ]	2740 ± 92	ITC [31]
		0	ACE [32]
		4374 ± 303	Fluo [31]
		3000 ± 50	Fluo [28, 29]
		0	ACE [40]
		1500 ± 100	C [30]
		2900 ± 60	<sup>19</sup> F NMR [30]
2921 ± 119	ITC [31]		
17	[C <sub>6</sub> mim][NTf <sub>2</sub> ]	3340 ± 140	ITC [34]
		9808 ± 565	ITC [31]
18	[C <sub>8</sub> mim][NTf <sub>2</sub> ]	12,069 ± 1088	ITC [31]

ACE affinity capillary electrophoresis, *C*<sub>2</sub>*mim* 1-ethyl-3-methylimidazolium, *C*<sub>4</sub>*mim* 1-butyl-3-methylimidazolium, *C*<sub>6</sub>*mim* 1-hexyl-3-methylimidazolium, *C*<sub>8</sub>*mim* 1-octyl-3-methylimidazolium, *C*<sub>10</sub>*mim* 1-decyl-3-methylimidazolium, *C*<sub>12</sub>*mim* 1-dodecyl-3-methylimidazolium, *Fluo* fluorescence displacement, *ITC* isothermal titration calorimetry, *NMR* nuclear magnetic resonance, *NTf*<sub>2</sub> triflimide

water molecules around their negative charges, avoiding all other inclusion patterns.

For the ILs [C<sub>12</sub>mim][PF<sub>6</sub>] and [C<sub>12</sub>mim][NTf<sub>2</sub>], the release of surrounding water molecules around the charged head results in the detachment of ion pairs, forming dissociated ions. Since these anions are sparingly water soluble and large, they might be included in  $\beta$ -CD. Such additional interactions should decrease the apparent binding affinity for C<sub>12</sub>mim, as a result of a possible competition with the dissociated ion pair but overwhelmingly in favor of the carbon chain. The predominance of the inclusion of the tail of the ILs is confirmed by the much higher association constants measured for [C<sub>8</sub>mim][PF<sub>6</sub>] and [C<sub>8</sub>mim][NTf<sub>2</sub>] (Table 1, entries 14 and 18) than those reported in the literature for the inclusion of the naked anions PF<sub>6</sub><sup>-</sup> and NTf<sub>2</sub><sup>-</sup> (average of 120 M<sup>-1</sup> and 2836 M<sup>-1</sup>, Table 1, entries 2 and 3).

Binding constants can also be dependent on the instrumental method used (Table 1). A comparative study revealed large variation and sometimes inconsistencies. As examples for study of the  $\beta$ -CD-[C<sub>4</sub>mim][NTf<sub>2</sub>] complex, six binding constants were reported, ranging from 1500 M<sup>-1</sup> to 4374 M<sup>-1</sup> (Table 1, entry 16), and for [C<sub>8</sub>mim][PF<sub>6</sub>] (Table 1, entry 14) binding affinity of 1177 M<sup>-1</sup> was obtained by fluorescence spectroscopy and 119,936 M<sup>-1</sup> was obtained by ITC. With the same experimental technique, small differences were noticed for [C<sub>4</sub>mim][NTf<sub>2</sub>] in fluorescence spectroscopy (4374 M<sup>-1</sup> and 3000 M<sup>-1</sup>) and ITC (2921 M<sup>-1</sup> and 3340 M<sup>-1</sup>) (Table 1, entry 16).

To extend the application fields of the CD-IL system, it is necessary to increase the amount of data to improve the prediction and to support the design of new supramolecular association complexes. We focused our study on the determination of new association constants using ACE. To validate the method used, the same investigations were performed by ITC analysis.

ACE is an online detection method and keeps the consumption of analytes and CD to a minimum [37]. Other advantages are the short analysis time, the absence of a solid phase, high versatility, and the possibility to customize the experimental conditions for specific needs. In 2004 Qi et al. [38] used for the first time the high conductivity and good solvating properties of [C<sub>4</sub>mim][BF<sub>4</sub>] as a running electrolyte in ACE to separate anthraquinones. After optimization, satisfactory separation and good sensitivity were obtained, validating this new analytical process. In 2007 François et al. [43] systematically studied the association constant with various CDs:  $\alpha$ -CD,  $\beta$ -CD,  $\gamma$ -CD, hydroxypropyl- $\alpha$ -CD, hydroxypropyl- $\beta$ -CD, hydroxypropyl- $\gamma$ -CD, heptakis(2,6-di-*O*-methyl)- $\beta$ -CD, and heptakis(2,3-tri-*O*-methyl)- $\beta$ -CD. Short IL chains with two or four carbon atoms did not form an inclusion complex because of their low lipophilic character inhibiting all affinity with the cavity of the CDs (Table 1, entries 8, 15, and 16). Only weak binding was observed with

$\alpha$ -CD. Longer carbon chain ( $C_8$ – $C_{12}$ ) ILs formed stable complexes (Table 1, entries 7, 9, and 10) with  $\beta$ -CD. This stability decreases with the size of the cavity because of the lack of strong interactions with the internal protons of the host. The stability of the complex is similar when  $\beta$ -CD or heptakis(2,6-di-*O*-methyl)- $\beta$ -CD is used and drastically decreases in the presence of heptakis(2,3-tri-*O*-methyl)- $\beta$ -CD. The synergistic CD–chiral IL system was also useful to separate neutral enantiomers in ACE by its taking part in the chiral recognition process through hydrogen bonding and steric hindrance [39].

## Materials and methods

$^1\text{H}$  (300-MHz) and  $^{13}\text{C}$  (75.5-MHz) NMR spectra were recorded with a Bruker ADVANCE 300 instrument at 23 °C. NMR was realized in a solution of an appropriate deuterated solvent, and the chemical shifts are described in parts per million relative to tetramethylsilane, with the residual peaks of the deuterated solvent as internal references. Coupling constants ( $J$ ) are given in hertz. The following abbreviations were used for the signals: s (singlet), d (doublet), t (triplet), m (multiplet). IR spectra were recorded with a PerkinElmer Fourier transform IR 1650 spectrometer. Electrospray ionization mass spectrometry data were acquired with an HCT Ultra ion trap mass spectrometer (Bruker Daltonics, Bremen, Germany). Elementary analyses were performed by the Service of Microanalyses of the Institut de Recherche en Chimie Organique Fine of Mont-Saint-Aignan.

## Chemical materials

$\beta$ -CD (purity greater than 98%), sodium tetraborate decahydrate, potassium acetate, and dimethyl sulfoxide were obtained from Sigma-Aldrich (Saint-Quentin-Fallavier, France). The ILs 1-dodecyl-3-methylimidazolium chloride [ $C_{12}\text{mim}$ ][Cl] [39], 1-dodecyl-3-methylimidazolium bromide [ $C_{12}\text{mim}$ ][Br] [39], 1-dodecyl-3-methylimidazolium iodide [ $C_{12}\text{mim}$ ][I] [40], 1-dodecyl-3-methylimidazolium hexafluorophosphate [ $C_{12}\text{mim}$ ][PF<sub>6</sub>] [39], and 1-dodecyl-3-methylimidazolium bis(trifluoromethylsulfonyl)imide [ $C_{12}\text{mim}$ ][NTf<sub>2</sub>] [39] were synthesized by the usual method as described in the literature. The analytical data were identical to those in the literature.

## Synthesis of 1-dodecyl-3-methylimidazolium acetate [ $C_{12}\text{mim}$ ][OAc]

[ $C_{12}\text{mim}$ ][Br] and potassium acetate were mixed in 2-propanol for 48 h. Insoluble potassium bromide was filtered. 2-Propanol was evaporated under a vacuum. The IL 1-dodecyl-3-methylimidazolium acetate [ $C_{12}\text{mim}$ ][OAc]

obtained was dissolved in cold acetone and filtered to remove all the residual potassium bromide [41].

$^1\text{H}$  NMR (300 MHz,  $\text{CD}_3\text{COCD}_3$ )  $\delta$  (ppm): 1.24 (3H, t,  $J = 6.5$  Hz,  $\text{N}(\text{CH}_2)_{11}\text{-CH}_3$ ), 1.63 (20H, s,  $-(\text{CH}_2)_{10}-$ ), 2.13 (3H, s,  $\text{CH}_3\text{CO}-$ ), 4.21 (3H, s,  $\text{N-CH}_3$ ), 4.51 (2H, t,  $^3J = 7.3$  Hz,  $\text{N-CH}_2\text{-C}_{11}\text{H}_{23}$ ), 7.74 (2H, d,  $J = 6.0$  Hz  $\text{-N-CH=CH-}$ ), 9.20 (1H, s,  $\text{-N}(\text{CH}_3)\text{-CH=N}(\text{C}_{12}\text{H}_{25})$ ).  $^{13}\text{C}$  NMR (75 MHz,  $\text{CD}_3\text{COCD}_3$ )  $\delta$  (ppm): 138.4, 124.6, 123.0 ( $\text{CH=CH}$ ), 50.2, 36.7, 32.6, 31.0, 30.7, 30.4, 30.2, 29.7, 29.4, 29.2, 26.9, 24.4, 23.3, 14.3. IR (attenuated total reflection D)  $\nu_{\text{max}}$  ( $\text{cm}^{-1}$ ): 3356.79, 2923.76, 2854.76, 1563.66, 1409.48. Positive electrospray ionization HRMS: calculated for  $\text{C}_{16}\text{H}_{31}\text{N}_2$   $m/z$  251.2487, found 251.2485.

## Affinity capillary electrophoresis method

ACE separates ionic species as a function of their charge/size and their friction force. The sample is injected into a capillary by capillarity, pressure, siphonage, or electroinjection. The migration of the analytes occurs through the application of an electric field between the electrodes. In the best experimental conditions all positive or negative ions are attracted inside the capillary by the electroosmotic flux to the cathodic detector. The cations are accelerated by the cathode, and the mobility of the anions is slowed by the anode. The analytes are separated during this migration by the difference in electrophoretic mobility due to in situ complexation and are detected at the exit of the capillary through an electropherogram as a function of time. ACE experiments were performed with a P/ACE MDQ capillary electrophoresis system (Beckman Coulter, Fullerton, CA, USA). An uncoated fused-silica capillary (Thermo Electron, Courtaboeuf, France), 31.2 cm long (21 cm to the detector) and with an inner diameter of 50  $\mu\text{m}$ , was used. The capillaries were thermostated at  $25.0 \pm 0.1$  °C. The samples were pressure-injected with 0.7 psi (50 mbar) for 5 s at the inlet side of the capillary (anode). Injections were repeated five times to check the precision of the data. Analytes were detected by UV absorbance at 214 nm. The 37 Karat program (version 8.0, Beckman Coulter) piloted the electrophoresis system and was used to obtain the data. All running electrolytes were prepared daily, without any prerequisite purification, with use of ultrapure water produced by means of a Milli-Q water purification apparatus (Millipore France, Montigny-le-Brotonneux, France). The solutions were sonicated just before use for 10 min. The running electrolytes contained borate or acetate salt according to the target pH (9.25 or 4.80 respectively) with an ionic strength of  $30 \times 10^{-3}$  M, and  $\beta$ -CD concentrations ranging from 0 to  $5 \times 10^{-3}$  M were used. Samples were prepared in borate or acetate solution at a concentration of  $2.5 \times 10^{-4}$  M or  $1.3 \times 10^{-3}$  M according to the samples. Because [ $C_{12}\text{mim}$ ][NTf<sub>2</sub>] is slightly insoluble in the electrolytes (borate and acetate) studied, 0.2% acetonitrile was added to the sample of the IL. New uncoated

capillaries were activated by the following washing process: water for 2 min, sodium hydroxide (1 M) for 30 min, and water for 10 min. The capillary was conditioned for 10 min with the electrolyte before the run and for 2 min between each run. The pH of the running solutions was measured before each experiment by a Cyberscan pH 510 instrument (Eutech Instruments Europe, Nijkerk, Netherlands). A Branson 2510 sonication apparatus (Branson, Danbury, C, USA) was used to degas all solutions.

In ACE mode, the sample contained a fixed amount of IL samples, and the running buffer contained various amounts of  $\beta$ -CD. The electrophoretic mobility of the injected analyte is dependent on the  $\beta$ -CD concentration [42]. As the  $\beta$ -CD concentration is increased in the running buffer, a viscosity correction was applied to the electrophoretic mobility according to François et al. [43]. The binding constant was estimated by at three linear least-squares plotting methods [*x*-reciprocal (Scatchard), *y*-reciprocal, or double-reciprocal plot]. For a 1:1 association complex, the change in solute mobility with changing ligand concentration is according to Eq. 1:

$$(\mu_i - \mu_f) / [CD] = -K(\mu_i - \mu_f) + K(\mu_c - \mu_f) \quad (1)$$

$$[CD] / (\mu_i - \mu_f) = [CD] / (\mu_c - \mu_f) + 1 / [K(\mu_c - \mu_f)] \quad (2)$$

$$1 / (\mu_i - \mu_f) = 1 / \{ (\mu_c - \mu_f) K [CD] \} + 1 / (\mu_c - \mu_f) \quad (3)$$

where  $\mu_i$  is the experimentally measured electrophoretic mobility of the solute,  $\mu_f$  is the mobility of the free (uncomplexed) solute,  $\mu_c$  is the electrophoretic mobility of the solute–ligand complex,  $K$  is the binding constant, and  $[CD]$  is the equilibrium ligand concentration. We also used a direct nonlinear curve fitting for constant determination with CurveExpert (version 1.4, Microsoft) and Eq. 4:

$$\mu_i = (\mu_f + \mu_c K [CD]) / (1 + K [CD]). \quad (4)$$

In the case of 1:2 complexation equilibrium, the effective mobility of the IL sample can be described by Eq. 5:

$$\mu_i = (\mu_f + \mu_c K [CD] + \mu_{c2} K K_2 [CD]^2) / (1 + K [CD] + K K_2 [CD]^2), \quad (5)$$

where  $\mu_f$ ,  $\mu_c$ , and  $\mu_{c2}$  are the mobility of the free (uncomplexed), 1:1 complexed, and 1:2 complexed forms of the IL respectively, and  $K_2$  is the formation constant of the 1:2 complex. When only 1:1 complexation occurs, Eq. 5 reduces to Eq. 4.

To determinate the stoichiometry of the CD–IL complexes, these two equations were applied to each system to confirm or rule out the 1:1 form.

## Isothermal titration calorimetry method

An isothermal calorimeter (ITC200, MicroCal, USA) was used to determine thermodynamic data for inclusion for each complex studied. The ILs were prepared in borate buffer at pH 9.30 or acetate buffer at pH 4.80 at a concentration of  $0.25 \times 10^{-3}$  M for  $[C_{12}mim][Cl]$  and  $[C_{12}mim][Br]$  and  $0.125 \times 10^{-3}$  M for  $[C_{12}mim][I]$ ,  $[C_{12}mim][PF_6]$ ,  $[C_{12}mim][NTf_2]$ , and  $[C_{12}mim][OAc]$ . They were titrated against  $2.5 \times 10^{-3}$  M solutions of  $\beta$ -CD in the same buffers at 25 °C. Titration experiments consisted in seven additions of the syringe solution to the cell content, with a first small aliquot of 1  $\mu$ L followed by six aliquots of 6  $\mu$ L (injection duration 12 s, time interval 90 s, agitation speed 1000 rpm). Heat flow was recorded as a function of time, the data for the first injection being discarded to eliminate any error induced by material diffusion effects between the two compartments or backlash in the drive screw mechanism of the syringe. The heat produced per injection was obtained by measuring each peak area, by means of the program Origin. Blank titrations were realized by injecting host, guest, or free buffer in a buffer solution. The effective binding signal was then obtained by subtraction of the data from each host and guest blank experiment from the data from the titration experiment and addition of the data from the buffer blank experiment (since this latter signal was already taken into account in each of the other blank experiments). Binding constants ( $K$ ,  $M^{-1}$ ) and inclusion enthalpies ( $\Delta H^\circ$ ,  $cal\ mol^{-1}$ ) were deduced from binding isotherms by nonlinear analyses of complexation heats as a function of total concentrations by means of a dedicated home-written program [44]. As  $Cl^-$ ,  $Br^-$ ,  $I^-$ , and  $AcO^-$  have negligible affinity for  $\beta$ -CD [45], the isotherms obtained for  $[C_{12}mim][Cl]$ ,  $[C_{12}mim][Br]$ ,  $[C_{12}mim][I]$ , and  $[C_{12}mim][OAc]$  were treated on the basis of a simple 1:1 stoichiometry. In contrast, as significant stability has been observed for  $\beta$ -CD complexes of  $PF_6^-$  and  $NTf_2^-$  [34], a competition model based on parallel inclusion of both the cationic part and the anionic part of  $[C_{12}mim][PF_6]$  and  $[C_{12}mim][NTf_2]$  was used to derive the thermodynamic data. Then, the inclusion entropy and free enthalpy were deduced from the values of  $K$  and  $\Delta H^\circ$ . Confidence intervals for each thermodynamic inclusion datum were obtained by the use of covariance matrices [44] resulting from global analysis of three independent measurements for each IL; the calculated standard deviations were multiplied by the corresponding Student *t* value (1.96).

## Results

### Affinity capillary electrophoresis analysis

The systematic study was performed by ACE with two electrolytes: acetate and borate buffers at pH 4.80 and pH 9.25

respectively [46]. In borate buffer, taking into account the uncertainties of the measurements, we obtained very similar association constants around  $11082 \text{ M}^{-1}$  for all the ILs:  $[\text{C}_{12}\text{mim}][\text{Cl}]$ ,  $[\text{C}_{12}\text{mim}][\text{Br}]$ ,  $[\text{C}_{12}\text{mim}][\text{I}]$ ,  $[\text{C}_{12}\text{mim}][\text{PF}_6]$ ,  $[\text{C}_{12}\text{mim}][\text{NTf}_2]$ , and  $[\text{C}_{12}\text{mim}][\text{OAc}]$  (Table 2, Fig. 2). In acetate buffer the association constants were all slightly less but still very similar whatever the nature of the counterion, from  $8400 \pm 1220 \text{ M}^{-1}$  for  $\text{PF}_6^-$  to  $7140 \pm 1190 \text{ M}^{-1}$  for  $\text{AcO}^-$ , and with an average of  $8160 \pm 1410 \text{ M}^{-1}$  (Table 2, Fig. 2). These data can be compared with the published association constants in sodium acetate buffer for the inclusion of  $[\text{C}_{12}\text{mim}][\text{BF}_4]$  in  $\beta$ -CD ( $10,994 \pm 600 \text{ M}^{-1}$ , Table 1, entry 10). According to the literature,  $\text{BF}_4^-$  and  $\text{Cl}^-$  anions cannot be included inside the cavity of  $\beta$ -CD (Table 1, entries 1, 4, and 8). Similarly, ILs with shorter alkyl chains such as  $[\text{C}_8\text{mim}][\text{Br}]$  ( $672 \pm 50 \text{ M}^{-1}$ , Table 1, entry 7) and  $[\text{C}_8\text{mim}][\text{Cl}]$  ( $624 \pm 43 \text{ M}^{-1}$ , Table 1, entry 6) have similar values. The association constants obtained by ACE for  $[\text{C}_{12}\text{mim}][\text{PF}_6]$ ,  $[\text{C}_{12}\text{mim}][\text{NTf}_2]$ , and  $[\text{C}_{12}\text{mim}][\text{OAc}]$  are quite similar in both buffers ( $8380 \pm 1950 \text{ M}^{-1}$  in borate buffer and  $7140 \pm 1090 \text{ M}^{-1}$  in acetate buffer for  $[\text{C}_{12}\text{mim}][\text{OAc}]$ , Table 2) and higher for halide anions in borate buffer ( $12,080 \pm 2400 \text{ M}^{-1}$  in borate buffer and  $7630 \pm 900 \text{ M}^{-1}$  in acetate buffer for  $[\text{C}_{12}\text{mim}][\text{I}]$ , Table 2). We believe that under these experimental conditions the electrolyte has an impact on the analysis because of the presence of a metathesis process. The acetate or borate ions are present in a very large excess and are able to exchange with the inorganic or organic anions, so the ILs present in solution are mostly in the acetate or borate forms.

The stoichiometry of CD–IL complexes was systematically checked by three linear least-squares plotting methods [ $x$ -reciprocal (Scatchard),  $y$ -reciprocal, or double-reciprocal plot] and also a direct nonlinear curve fitting (Eqs. 1–3; see the [Electronic supplementary material](#)), and the formation of the

1:1 complex was observed for  $[\text{C}_{12}\text{mim}][\text{Cl}]$ ,  $[\text{C}_{12}\text{mim}][\text{Br}]$ ,  $[\text{C}_{12}\text{mim}][\text{I}]$ ,  $[\text{C}_{12}\text{mim}][\text{PF}_6]$ , and  $[\text{C}_{12}\text{mim}][\text{OAc}]$ . For  $[\text{C}_{12}\text{mim}][\text{NTf}_2]$ , the coefficients obtained were not optimal but Eq. 5 led to the same 1:1 stoichiometry. The correlation coefficients obtained are given in the electronic supplementary material.

### Isothermal titration calorimetry analysis

ITC is a very sensitive technique for determining simultaneously the stoichiometry, binding constant, enthalpy, and entropy of complex formation. As any complexation occurring within the ITC cell might be detected, it is important to take the real equilibrium model into account. When an absence of metathesis was postulated, some discrepancies between theoretical and experimental isotherms were observed in the case of  $[\text{C}_{12}\text{mim}][\text{NTf}_2]$  and  $[\text{C}_{12}\text{mim}][\text{OAc}]$ . Since  $\text{PF}_6^-$  and  $\text{NTf}_2^-$  (in contrast to  $\text{Br}^-$ ,  $\text{Cl}^-$ ,  $\text{I}^-$ , and  $\text{AcO}^-$ ) have significant affinity for  $\beta$ -CD, the ITC isotherms for  $[\text{C}_{12}\text{mim}][\text{NTf}_2]$  and  $[\text{C}_{12}\text{mim}][\text{OAc}]$  are expected to contain heat corresponding to parallel inclusion of both the organic cation and the inorganic anion. To take into account such independent complexation of the cationic and anionic parts of ILs, a 1:1 competitive model was used to treat the binding isotherms. Perfect fits were then obtained when we considered a total metathesis for each IL, in the presence of each buffer. Corresponding thermodynamic data are presented in Table 2.

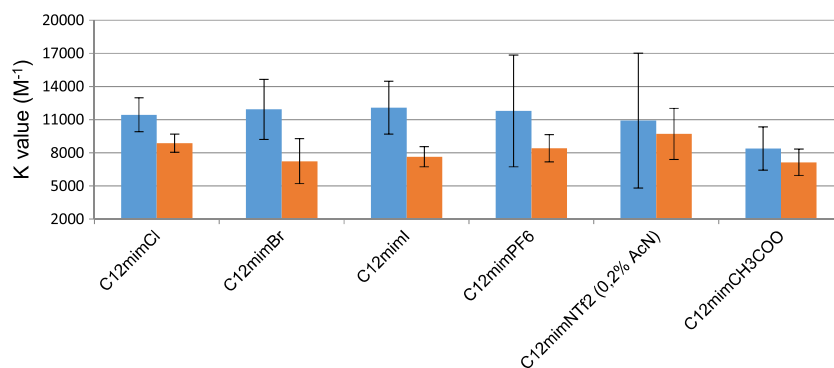
No significant difference in binding affinity (average approximately  $20,000 \text{ M}^{-1}$ ) was observed for  $[\text{C}_{12}\text{mim}][\text{Cl}]$ ,  $[\text{C}_{12}\text{mim}][\text{Br}]$ ,  $[\text{C}_{12}\text{mim}][\text{I}]$ ,  $[\text{C}_{12}\text{mim}][\text{PF}_6]$ ,  $[\text{C}_{12}\text{mim}][\text{NTf}_2]$ , and  $[\text{C}_{12}\text{mim}][\text{OAc}]$ , whatever buffer was used (Fig. 3). In addition, if the formation constants in borate buffer are systematically inferior to those in acetate buffer for each IL, the calculated confidence intervals do not

**Table 2** Affinity capillary electrophoresis (ACE) and isothermal titration calorimetry (ITC) results in borate and acetate buffer with various ionic liquids and  $\beta$ -cyclodextrin at 298 K

	Buffer	ACE	ITC		
		$K (\text{M}^{-1})$	$K (\text{M}^{-1})$	$\Delta H (\text{cal mol}^{-1})$	$-T\Delta S (\text{cal mol}^{-1} \text{K}^{-1})$
$[\text{C}_{12}\text{mim}][\text{Cl}]$	Acetate	$8850 \pm 820$	$21,600 \pm 2538$	$-2053 \pm 51$	$-3854 \pm 121$
	Borate	$11,430 \pm 1530$	$18,006 \pm 2001$	$-2243 \pm 57$	$-3556 \pm 123$
$[\text{C}_{12}\text{mim}][\text{Br}]$	Acetate	$7230 \pm 2030$	$22,484 \pm 2475$	$-2177 \pm 51$	$-3753 \pm 116$
	Borate	$11,920 \pm 2720$	$17,405 \pm 1897$	$-2303 \pm 59$	$-3476 \pm 124$
$[\text{C}_{12}\text{mim}][\text{I}]$	Acetate	$7630 \pm 900$	$20,803 \pm 2419$	$-2102 \pm 71$	$-3782 \pm 140$
	Borate	$12,080 \pm 2400$	$18,651 \pm 2062$	$-2209 \pm 74$	$-3611 \pm 140$
$[\text{C}_{12}\text{mim}][\text{PF}_6]$	Acetate	$8400 \pm 1220$	$22,644 \pm 2818$	$-1969 \pm 69$	$-3966 \pm 143$
	Borate	$11,780 \pm 5050$	$19,711 \pm 2168$	$-2221 \pm 73$	$-3632 \pm 138$
$[\text{C}_{12}\text{mim}][\text{NTf}_2]$	Acetate	$9690 \pm 2320$	$21,324 \pm 2675$	$-1949 \pm 71$	$-3950 \pm 145$
	Borate	$10,900 \pm 6110$	$18,596 \pm 2205$	$-2060 \pm 74$	$-3758 \pm 145$
$[\text{C}_{12}\text{mim}][\text{OAc}]$	Acetate	$7140 \pm 1190$	$19,302 \pm 2279$	$-2068 \pm 73$	$-3772 \pm 143$
	Borate	$8380 \pm 1950$			

*C*<sub>12</sub>mim 1-dodecyl-3-methylimidazolium

**Fig. 2** Association constants obtained by affinity capillary electrophoresis for ionic liquids **1a–1f** in borate buffer (blue) and acetate buffer (orange)



demonstrate a significant variation between the two media. For all ILs, the formation of an inclusion complex is a spontaneous process characterized by low enthalpic stabilization, reinforced by favorable entropic gain, in both buffers.

## Discussion

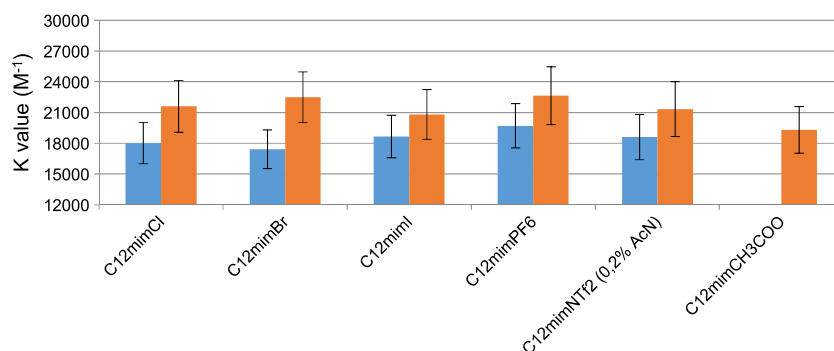
Metathesis reactions of  $[C_{12}mim][Cl]$ ,  $[C_{12}mim][Br]$ ,  $[C_{12}mim][I]$ ,  $[C_{12}mim][PF_6]$ ,  $[C_{12}mim][NTf_2]$ , and  $[C_{12}mim][OAc]$  in acetate or borate buffers during ACE and ITC experiments were observed. This conclusion is supported by the results obtained by François et al. [43] with shorter-chain ILs. In acetate buffer no formation of an inclusion complex with  $\beta$ -CD was detected by ACE in the presence of  $[C_2mim][NTf_2]$  and  $[C_4mim][NTf_2]$  (Table 1, entries 15 and 16), whereas high association constants (in the 1500–4500- $M^{-1}$  range) for  $[C_4mim][NTf_2]$  with  $\beta$ -CD were reported with use of other analytical methods such as fluorescence displacement, NMR spectroscopy, conductimetry, and ITC (Table 1, entries 15 and 16). The lipophilicity of the  $NTf_2^-$  counterion is much higher than that of the two or four carbon atom chains of the imidazolium. Thus the exchange of the  $NTf_2^-$  counteranion with acetate anion can explain this lack of detection observed and confirm our results. So the necessity to use ionic electrolytes in ACE limits the application of this technique to evaluate the influence of anions on the association constants of imidazolium-based ILs with CDs. ITC analysis conducted in a neutral medium could circumvent such a limitation, but in the

absence of a buffer, nonspecific heat produced by any pH variation would lead to wrong measurement of formation constants.

The ITC binding constants are greater than those obtained by ACE measurements (10000  $M^{-1}$  higher) (Figs. 2 and 3). In 2008 Parker and Stalcup [47] reported a simultaneous study using ITC and ACE to separated fatty acid and  $\beta$ -CD. They noticed the same order of magnitude with also greater binding affinity with ITC. However, another study of a succinate derivative and CDs provided similar results with three techniques (ACE, ITC, and NMR spectroscopy) [48]. We reported binding constants for various  $\beta$ -CDs and 2-anilino-6-naphthalenesulfonate guest and noticed that the fluorescence-based measurements were consistently greater than those obtained by ACE [49]. During the fluorescence experiment the  $S_1$  excited state of the guest is detected. If the excited-state lifetime is long relative to the rates of exit of the guest from and entry of the guest into the cavity, the fluorescence results will yield the binding constant of the guest in its excited state rather than that in its ground state. By contrast, the electrophoresis analysis determines the binding of the ground state of the guest.

To evaluate the reason for the discrepancies observed in this work, the concentration effect was studied. Although no significant variation was obtained with ITC by modification of the concentration or inversion of the titrant/titrant solution, we observed with ACE an increase of the association constants with a decrease of the concentration of the sample. The heat recorded in ITC analysis corresponds to the difference between

**Fig. 3** Association constants obtained by isothermal titration calorimetry for ionic liquids **1a–1f** in borate buffer (blue) and acetate buffer (orange)





two well-defined equilibrium states, but in ACE experiments the dynamic equilibrium between the free and the complexed forms evolves all along the course of the analyte within the capillary. As this perturbation depends on the concentration, the measured binding strength may vary with this parameter.

To optimize the ACE experimental conditions, the influence of applied pressure, temperature, and ionic strength of the electrolyte was studied for  $[C_{12}mim][PF_6]$ . The pressure had a weak effect, whereas the temperature and the ionic strength had a nonnegligible impact on the complexation mechanism as expected in the presence of a dynamic equilibrium. The binding affinity decreased when the temperature increased because of higher instability. From the results it clearly appeared that the experimental conditions are very important and can affect the observed association constants very drastically. The concentration of the sample is the major parameter that influences the rate of the formation of the complex in ACE. The other parameters, such as temperature, pressure, electrolyte (nature, ionic force), and capillary (nature, length, and diameter), are less influential but have a key effect on the symmetry of the peaks and the speed of analysis. The constants were extracted from the electrophoretic mobilities corresponding to the times associated with the exit peaks. However, if the peaks are not perfectly symmetrical, because of too strong a concentration of the sample or because of electromigration dispersion, the values can be skewed as previously shown by Lynen et al. [50], Le Saux et al. [51], and Steinbock et al. [52]. The concentration of the IL as a function of the CD concentration has to be as low as possible to reach an infinite-dilution state. Only in this condition can the equilibrium occur as quickly as in an ITC experiment. However, technically ACE has limits of concentration and UV detection, leading to higher uncertainty. The limit of detection in ACE usually used is a signal-to-noise ratio greater than 3. Under the experimental conditions used in this work, the quantities of IL injected into the capillary were about  $2 \times 10^{-15}$  mol for a CD content in the electrolyte of  $3.5 \times 10^{-9}$  mol. The difference between these two quantities seems insufficient to approach infinite dilution. But the limit of detection does not enable us to decrease the concentration of the IL. We thus reach the limits of this method of determination.

## Conclusion

A new classification by counteranion of the association constants reported in the literature and in this work was established. The results showed heterogeneous data according to the experimental processes. We investigated the binding interactions of complexes with the  $\beta$ -CD cavity and six ILs based on the 1-dodecyl-3-methylimidazolium cation by two complementary techniques, ACE and ITC, in the presence of acetate buffer or borate buffer. We showed that such basic or acidic medium has to be avoided in this case because of an ion

metathesis reaction between the IL and the buffer. Systematic comparison of the results between these two techniques underlined the major influence of the sample concentration. We observed greater binding constants in ITC experiments than in ACE experiments. This study gathered the data collected in the literature and will help to select the tail length of the IL and the nature of the counteranion to design innovative smart materials based on this synergic system [7–17].

**Acknowledgments** The authors thank Claudette Martin from Rouen University for the analysis of the ionic liquids.

## Compliance with ethical Standards

**Conflict of interest** The authors declare that they have no conflict of interest.

## References

1. D'Souza VT, Lipkowitz KB. Cyclodextrins: introduction. *Chem Rev.* 1998;98:1741–2.
2. Kenneth AC. Binding constants: the measurement of molecular complex stability. 1st ed. Oxford: Wiley-Interscience; 1987.
3. Huddleston JG, Visser AE, Reichert WM, Willauer HD, Broker GA, Rogers RD. Characterization and comparison of hydrophilic and hydrophobic room temperature ionic liquids incorporating the imidazolium cation. *Green Chem.* 2001;3:156–64.
4. Hallett JP, Welton T. Room-temperature ionic liquids: solvents for synthesis and catalysis 2. *Chem Rev.* 2011;111:3508–76.
5. Anderson JL, Ding J, Welton T, Armstrong DW. Characterizing ionic liquids on the basis of multiple solvation interactions. *J Am Chem Soc.* 2002;124:14247–54.
6. Rogalski M, Modaressi A, Magri P, et al. Physico-chemical properties and phase behavior of the ionic liquid- $\beta$ -cyclodextrin complexes. *Int J Mol Sci.* 2013;14:16638–55.
7. Mahlambi MM, Malefetse TJ, Mamba BB, Krause RWM. Polymerization of cyclodextrin-ionic liquid complexes for the removal of organic and inorganic contaminants from water. In: Korkorin A, editor. *Ionic liquids: applications and perspectives.* Rijeka: InTech; 2011. p. 115–51.
8. Duri S, Tran CD. Supramolecular composite materials from cellulose, chitosan, and cyclodextrin: facile preparation and their selective inclusion complex formation with endocrine disruptors. *Langmuir.* 2013;29:5037–49.
9. Raoov M, Mohamad S, Abas MR. Synthesis and characterization of  $\beta$ -cyclodextrin functionalized ionic liquid polymer as a macroporous material for the removal of phenols and arsenic (V). *Int J Mol Sci.* 2014;15:100–19.
10. Amajjahe S, Munteanu M, Ritter H. Switching the solubility of PMMA bearing attached cyclodextrin-moieties by supramolecular interactions with ionic liquids. *Macromol Rapid Commun.* 2009;30:904–8.
11. Leclercq L, Lacour M, Sanon SH, Schmitzer AR. Thermoregulated microemulsions by cyclodextrin sequestration: a new approach to efficient catalyst recovery. *Chem Eur J.* 2009;15:6327–31.
12. Li S, Xing P, Hou Y, Yang J, Yang X, Hao BA. Formation of a sheet-like hydrogel from vesicles via precipitates based on an ionic liquid-based surfactant and  $\beta$ -cyclodextrin. *J Mol Liq.* 2013;188:74–80.

13. Zhang J, Shen X. Temperature-induced reversible transition between vesicle and supramolecular hydrogel in the aqueous ionic liquid- $\beta$ -cyclodextrin system. *J Phys Chem B*. 2013;117:1451–7.
14. Jiangna G, Chao Y, Mingyu G, Lei W, Feng Y. Flexible and voltage-switchable polymer velcro constructed using host-guest recognition between poly(ionic liquid) strips. *Chem Sci*. 2014;5:3261–6.
15. Zhou Z, Li X, Chen X, Hao X. Synthesis of ionic liquids functionalized  $\beta$ -cyclodextrin-bonded chiral stationary phases and their applications in high-performance liquid chromatography. *Anal Chim Acta*. 2010;678:208–14.
16. Huang K, Zhang X, Armstrong DW. Ionic cyclodextrins in ionic liquid matrices as chiral stationary phases for gas chromatography. *J Chromatogr A*. 2010;1217:5261–73.
17. Stalcup AM, Cabovska B. Ionic liquids in chromatography and capillary electrophoresis. *J Liq Chromatogr*. 2004;27:1443–59.
18. Mendes A, Branco LC, Morais C, Simplicio AL. Electroosmotic flow modulation in capillary electrophoresis by organic cations from ionic liquids. *Electrophoresis*. 2012;33:1182–90.
19. Tran CD, De Paoli Lacerda S. Near-infrared spectroscopic investigation of inclusion complex formation of cyclodextrins in room-temperature ionic liquid. *J Incl Phenom Macrocycl Chem*. 2002;44:185–90.
20. Gao YA, Li ZH, Du JM, et al. Preparation and characterization of inclusion complexes of  $\beta$ -cyclodextrin with ionic liquid. *Chem Eur J*. 2005;11:5875–80.
21. He Y, Shen X. Interaction between  $\beta$ -cyclodextrin and ionic liquids in aqueous solutions investigated by a competitive method using a substituted 3H-indole probe. *J Photochem Photobiol A*. 2008;197:253–9.
22. Rak J, Ondo D, Tkadlecova M, Dohnal V. On the interaction of ionic liquid 1-butyl-3-methylimidazolium hexafluorophosphate with  $\beta$ -cyclodextrin in aqueous solutions. *Z Phys Chem*. 2010;224:893–906.
23. Zhang J, Shen X. Multiple equilibria interaction pattern between the ionic liquids CnmimPF<sub>6</sub> and  $\beta$ -cyclodextrin in aqueous solutions. *J Phys Chem B*. 2011;115:11852–61.
24. Li HG, Zhang Q, Liu M, Liu J, Sun DZ. Studies on interaction of ionic liquids with cyclodextrins in aqueous solution. *Indian J Chem*. 2010;49A:752–6.
25. Roy MN, Roy MC, Roy K. Investigation of an inclusion complex formed by ionic liquid and  $\beta$ -cyclodextrin through hydrophilic and hydrophobic interactions. *RSC Adv*. 2015;5:56717–23.
26. Amajjahe S, Choi S, Munteanu M, Ritter H. Pseudopolyanions based on poly(NIPAAM-co- $\beta$ -cyclodextrin methacrylate) and ionic liquids. *Angew Chem Int Ed*. 2008;47:3435–7.
27. Hodyna D, Bardeau JF, Metelytsia L, et al. Efficient antimicrobial activity and reduced toxicity of 1-dodecyl-3-methylimidazolium tetrafluoroborate ionic liquid/ $\beta$ -cyclodextrin complex. *Chem Eng J*. 2016;284:1136–45.
28. Gao Y, Zhao X, Dong B, Zheng L, Li N, Zhang S. Inclusion complexes of  $\beta$ -cyclodextrin with ionic liquid surfactants. *J Phys Chem B*. 2006;110:8576–81.
29. Li N, Liu J, Zhao X, et al. Complex formation of ionic liquid surfactant and  $\beta$ -cyclodextrin. *Colloids Surf A*. 2007;292:196–201.
30. He Y, Chen Q, Xu C, Zhang J, Shen X. Interaction between ionic liquids and  $\beta$ -cyclodextrin: a discussion of association pattern. *J Phys Chem B*. 2009;113:231–8.
31. Zhang J, Shi J, Shen X. Further understanding of the multiple equilibria interaction pattern between ionic liquid and  $\beta$ -cyclodextrin. *J Incl Phenom Macrocycl Chem*. 2014;79:319–27.
32. Semino R, Rodríguez J. Molecular dynamics study of ionic liquids complexation within  $\beta$ -cyclodextrins. *J Phys Chem B*. 2015;119:4865–72.
33. Funasaki N, Ishikawa S, Neya S. 1:1 and 1:2 complexes between long-chain surfactant and  $\alpha$ -cyclodextrin studied by NMR. *J Phys Chem B*. 2004;108:9593–8.
34. Ondo D, Tkadlecova M, Dohnal V, et al. Interaction of ionic liquids ions with natural cyclodextrins. *J Phys Chem B*. 2011;115:10285–97.
35. Hayes R, Warr GG, Atkin R. Structure and nanostructure in ionic liquids. *Chem Rev*. 2015;115:6357–426.
36. Lungwitz R, Spange S. A hydrogen bond accepting (HBA) scale for anions, including room temperature ionic liquids. *New J Chem*. 2008;32:392–4.
37. Schou C, Heegaard NH. Recent applications of affinity interactions in capillary electrophoresis. *Electrophoresis*. 2006;27:44–59.
38. Qi S, Cui S, Chen X, Hu Z. Rapid and sensitive determination of anthraquinones in Chinese herb using 1-butyl-3-methylimidazolium-based ionic liquid with  $\beta$ -cyclodextrin as modifier in capillary zone electrophoresis. *J Chromatogr A*. 2004;1059:191–8.
39. Aupoix A, Pegot B, Vo-Thanh G. Synthesis of imidazolium and pyridinium-based ionic liquids and application of 1-alkyl-3-methylimidazolium salts as pre-catalysts for the benzoin condensation using solvent-free and microwave activation. *Tetrahedron*. 2010;66:1352–6.
40. Wang M, Pan X, Xia S, Zhang C, Li W, Dai S. Regulating mesogenic properties of ionic liquid crystals by preparing binary or multi-component systems. *J Mater Chem*. 2012;22:2299–305.
41. Rodriguez-Palmeiro I, Rodriguez-Escontrela I, Rodriguez O, Arce A, Soto A. Characterization and interfacial properties of the surfactant ionic liquid 1-dodecyl-3-methyl imidazolium acetate for enhanced oil recovery. *RSC Adv*. 2015;5:37392–8.
42. Liu Y, Shamsi SA. Combined use of chiral ionic liquid surfactants and neutral cyclodextrins: evaluation of ionic liquid head groups for enantioseparation of neutral compounds in capillary electrophoresis. *J Chromatogr A*. 2014;1360:296–304.
43. François Y, Varenne A, Sirieix-Plenet J, Gareil P. Determination of aqueous inclusion complexation constants and stoichiometry of alkyl(methyl)-methylimidazolium-based ionic liquid cations and neutral cyclodextrins by affinity capillary electrophoresis. *J Sep Sci*. 2007;30:751–60.
44. Bertaut E, Landy D. Improving ITC studies of cyclodextrin inclusion compounds by global analysis of conventional and non-conventional experiments. *Beilstein J Org Chem*. 2014;10:2630–41.
45. Connors KA. Measurement of cyclodextrin complex stability constants. *Compr Supramol Chem*. 1996;3:205–41.
46. Tanaka Y, Terabe S. Estimation of binding constants by capillary electrophoresis. *J Chromatogr B*. 2002;768:81–92.
47. Parker KM, Stalcup AM. Affinity capillary electrophoresis and isothermal titration calorimetry for the determination of fatty acid binding with beta-cyclodextrin. *J Chromatogr A*. 2008;1204:171–82.
48. Danel C, Duval C, Azaroual N, et al. Complexation of triptolide and its succinate derivative with cyclodextrins: affinity capillary electrophoresis, isothermal titration calorimetry and <sup>1</sup>H NMR studies. *J Chromatogr A*. 2011;1218:8708–14.
49. Favrelle A, Gouhier G, Guillen F, et al. Structure-binding effects: comparative binding of 2-anilino-6-naphthalenesulfonate by a series of alkyl- and hydroxyalkyl-substituted  $\beta$ -cyclodextrins. *J Phys Chem B*. 2015;119:12921–30.
50. Lynen F, Borremans F, Sandra P. Practical evaluation of the influence of excessive sample concentration on the estimation of dissociation constants with affinity capillary electrophoresis. *Electrophoresis*. 2001;22:1974–8.
51. Le Saux T, Varenne A, Gareil P. Peak shape modeling by Haarhoff-Van der Linde function for the determination of correct migration times: a new insight into affinity capillary electrophoresis. *Electrophoresis*. 2005;26:3094–104.
52. Steinbock B, Vichaikul PP, Steinbock O. Nonlinear analysis of dynamic binding in affinity capillary electrophoresis demonstrated for inclusion complexes of  $\beta$ -cyclodextrin. *J Chromatogr A*. 2001–2002;943:139–46.